Available online at www.sciencedirect.com
ScienceDirect
Ceramics International 35 (2009) 2017–2022
CERAMICS INTERNATIONAL
www.elsevier.com/locate/ceramint

An evaluation of plasma-sprayed coatings based on Al_2O_3 and Al_2O_3–13 wt.% TiO_2 with bond coat on pure titanium substrate

Şenol Yılmaz *

Sakarya University, Engineering Faculty, Department of Metallurgical and Material Engineering, 54187 Esentepe Campus, Sakarya, Turkey

Received 15 March 2008; received in revised form 25 October 2008; accepted 9 November 2008
Available online 11 December 2008

Abstract

In this study, the effects of bond coat on the properties of Al_2O_3 and Al_2O_3–13 wt.% TiO_2 coatings, which is plasma sprayed onto a commercial pure titanium substrate with and without Ni–5 wt.% Al (METCO 450 NS) as bond coating layer were investigated in terms of microhardness, bonding strength and surface roughness. Optical and scanning electron microscopy (SEM) examinations revealed that there is a uniform coating layer with no spalling and delamination. However, there is a little amount of porosity. The results indicated that the application of bond coat layer in the plasma spraying of Al_2O_3 and Al_2O_3–13 wt.% TiO_2 on pure titanium substrate has increased the hardness and bonding strength of coatings. While the adhesive bonding is dominant without bond coat, the cohesive bonding is dominant with the application of the bond coating layer. It has been observed that percentage of cohesion strength was about three times higher than that of adhesion strength.

Keywords: B. Porosity; C. Mechanical properties; D. Al_2O_3; E. Biomedical applications

1. Introduction

Ceramic materials with high hardness and high resistance to thermal and corrosive conditions and relatively low densities offer many advantages over metallic and polymeric materials [1,2]. Oxide ceramics such as alumina, zirconia, titania, chromia, silica and yttria have been used widely as surface coating materials to improve wear, erosion, cavitation, fretting and corrosion resistance [1] and to provide lubrication and thermal insulation [3]. They are especially useful in applications where wear and corrosion resistances are required simultaneously. Thermal spraying techniques represent a group of widely used processes for the production of various overplayed protective coatings to improve the surface characteristics of materials. Plasma spraying is a widely used method among the thermal spray processes [1,4–7].

It is well known that one of the main concerns when using plasma-spray techniques is the determination of the coating to substrate adhesion [8]. The main mechanism of the coating–substrate adhesion in conventional plasma spraying is mechanical interlocking. The irregularities of a rough surface are filled with the spreading molten materials due to the impact pressure. The subsequent solidification leads to mechanical interlocking or 'keying' [9]. The mismatch between the thermal expansion coefficients of ceramic and metals leads to the development of excessive stresses at the interface, which is the main cause of problems in metal–ceramic joining. This is a common problem for depositing ceramic coating on metals [10]. To solve that problem is to use a metallic bond coat onto the substrate for better interface adherence of the coating [10,11]. Bond coatings are used widely in many industrial plasma-spray applications. They have specific functions; because the substrate and the main coating have different coefficient of thermal expansion, bond coating layer should be used to provide a good thermal expansion match between these two different layers. Bond coatings are always thinner than the main coatings [12,13].

Ti and Ti-based alloys are widely used in several fields of bone substitution due to their biocompatibility, high corrosion resistance and good mechanical properties [14,15]. These alloys possess some excellent properties, including low density, high strength, and corrosion resistance [16]. Many kinds of prosthetic implants have been developed for both orthopedic and dental applications. Ti and Ti-based alloys can be coated

* Tel.: +90 264 2955768; fax: +90 264 2955601.
E-mail addresses: symaz@sakarya.edu.tr, symaz68@gmail.com.

0272-8842/$34.00 © 2008 Elsevier Ltd and Techna Group S.r.l. All rights reserved.
doi:10.1016/j.ceramint.2008.11.017

using different methods, such as conventional enameling, sputtering techniques and plasma spray [14,15]. The as-obtained implants can offer several advantages, in terms of the high mechanical properties of the metallic substrate combined with coating. Moreover, a good protection of the substrate from corrosion and biological fluids is provided [14].

The aim of this study is to find out the effect of bond coat application on mechanical properties and microstructural characteristic of Al_2O_3 and Al_2O_3–13 wt.% TiO_2 coatings on titanium. Al_2O_3 and Al_2O_3–13 wt.% TiO_2 coatings increase corrosion, wear resistance and beneficial bioreactivity in biomedical applications. The coatings were characterized by X-ray diffraction (XRD), optical microscopy, scanning electron microscopy (SEM) and a Vickers microhardness tester. Bonding strength of coatings was tested using adhesion test ASTM C-633.

2. Experimental details

2.1. Substrate and coatings

The substrate used for the coatings was the commercial pure titanium with the dimensions of 20 mm in diameter and 10 mm in height. The composition (wt.%) of substrate was N: 0.02, C: 0.08, H: 0.007, Fe: 0.18, O: 0.15 and Ti as the balance. The substrates were prepared metallographically by polishing with 1000 grid emery paper at the final stage. The surface of Ti-substrates was grit-blasted to provide surface roughness for better adherence between the coating and metallic substrate with 35 grid Al_2O_3 under 0.2 MPa pressure and a flow rate of 2 kg min^{-1}. Grit blasting was realized at the 45° with 50 mm distance to the substrate surface (because sand particles can get away from the surface without impressing elastically and not turn back to the nozzle). The grid blasting machine is manual grit blasting equipment of Cetingil made with 8 mm WC nozzle. The resulting average roughness of the substrate surface (R_a) after grid blasting that measured Perthometer M4P surface roughness tester is between 3.8 and 4.8 μm.

This was followed by an ultrasonic cleaning in ethyl alcohol using acetone solvent for 15 min and dried. A distance of 100 mm was chosen between the gun and substrate during the deposition of the coating powders. Alumina (METCO 105 NS) and alumina–13 wt.% TiO_2 (METCO 130 SF) coatings were produced using an atmospheric plasma-spraying (APS) technique on titanium with and without bond coating. Ni–5 wt.% Al (METCO 450 NS) was used for the bond layer. The plasma-spraying parameters and the plasma-spray powder particle sizes are given in Tables 1 and 2. The torch nozzle used for coatings was METCO 3 MB with 6 mm alloyed Cu nozzle. The position of the injector relative to the nozzle exit was 90°. The injector is in the same axis with torch. Powder unit of injector was METCO 3 MP powder feed unit. The coating operations were performed in the room temperature.

In this study, the critical plasma-spray parameter (CPS) was approximately 1000, and is defined by [7,13,17]:

$$CPS = \frac{\text{voltage} \times \text{current}}{\text{primary gas (Ar) flow rate}} \quad (1)$$

Table 1
Plasma-spray coating parameters of Ni–5 wt.% Al bond layer, Al_2O_3 and Al_2O_3–13 wt.% TiO_2 ceramic coatings.

Parameters (units)	Ni–5 wt.% Al coating	Al_2O_3 coatings	Al_2O_3–13 wt.% TiO_2 ceramic coatings
Plasma gun	3 MB	3 MB	3 MB
Current (A)	500	500	500
Voltage (V)	64–70	75	70–75
Gas flow for Ar (l/min)	27	40	40
Gas flow for H_2 (l/min)	14	14	14
Spray distance (mm)	130	100	100
Powder feed rate (g/min)	34	39	39
Carrier gas flow (l/min)	3–6	2–6	2–6

Table 2
The plasma-spray powder particles size.

Plasma-spray powders	Particle size (μm)
Pure Al_2O_3	−20 + 5
Al_2O_3–13 wt.% TiO_2	−30 + 5
Ni–5 wt.% Al (bond coat)	−88 + 45

2.2. Characterization

XRD analysis was conducted with a RIGAKU D/MAX-2200/PC type difractometer with a Cu Kα radiation, which has a wavelength of 1.54059 Å to analyze phases present in the coatings, qualitatively. Optical microscope (Olympus BHM 313 U) and scanning electron microscopy (JEOL 6060 LV) were used to study the microstructure and morphology of the coatings. The hardness of coating layer and bond coat were measured on the polished cross-sections of the samples using a Vickers microhardness tester (FutureTech FM 700) with a load of 100 gf. Indenting time of the Vickers indenter was applied for 10 s. Bonding strength of coatings was tested using adhesion test ASTM C-633. The coating layer was glued on the pull rods using an epoxy adhesive which was cured for 24 h at room temperature. All tests were carried out by using a tensile machine under ambient conditions with a cross-head speed of 0.5 mm min^{-1} to determine bond strength. In addition, pull rods were also glued directly to each other and measured the strength of the epoxy. The bonding type of coatings and the percentage of adhesion and cohesion were calculated by the measurement of the separation percents of coating on surface using a planemeter.

3. Results and discussion

3.1. Microstructure

Figs. 1–3 show the microstructure of the Al_2O_3 and Al_2O_3–13 wt.% TiO_2 coatings produced by atmospheric plasma spray. In all the coatings, some pores and splat boundaries are observed. The ceramic layer and bond layer mainly display a lamellar structure, in which the lamellar of both the ceramic layer and bond coat layer are almost parallel to the substrate

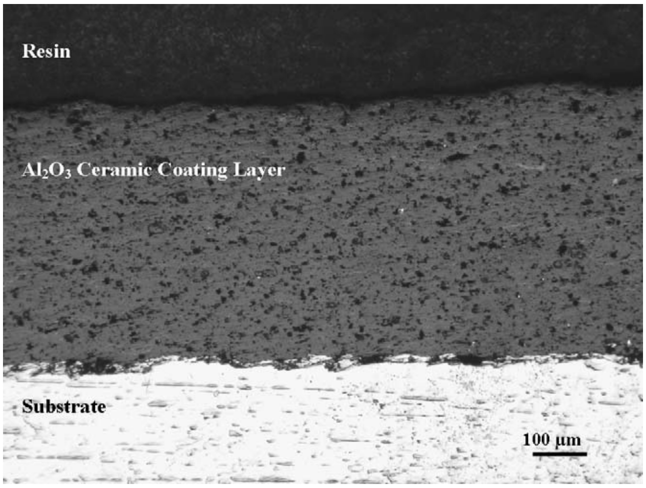

Fig. 1. Optical micrograph of cross-section view for the Al_2O_3 coating on titanium.

(a)
(b)

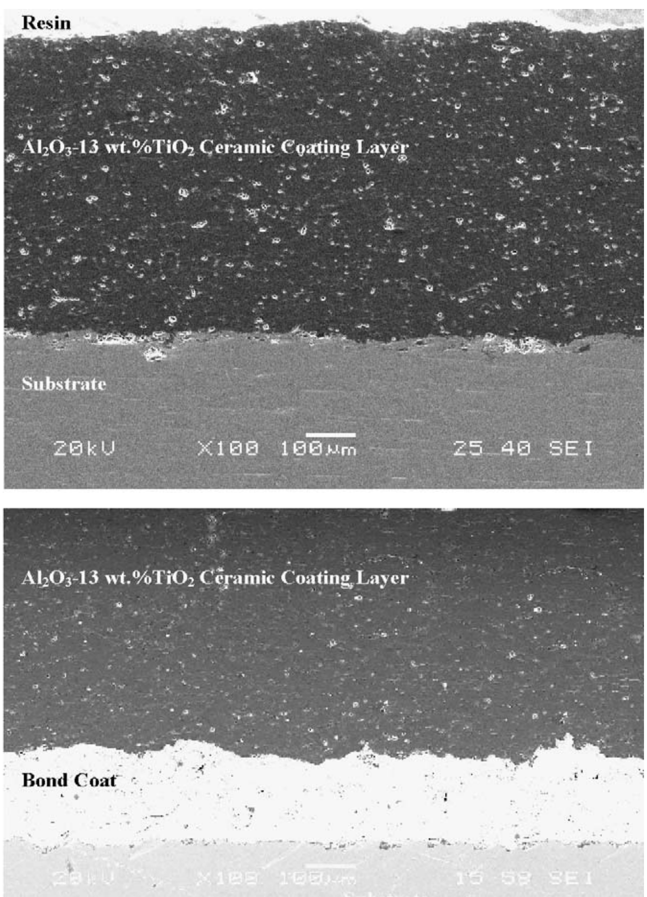

Fig. 2. SEM micrograph of cross-section view for the Al_2O_3–13 wt.% TiO_2 coating on titanium. (A) Without bond coat and (B) with bond coat.

surface. It is well known that the microstructure of thermal spray coating is characterized by lamellar structure. The difference of microstructural features of the coatings from the conventionally processed bulk materials makes them behave mechanically in a different way [18]. It is probable that, thermally grown oxides are thought to grow due to the oxidation of aluminum in the plasma flame and during splat formation [13]. Partially melted powders and porosity are detected in coatings as indicated by arrows in Fig. 3. As previously reported that plasma-spray coatings usually contain porosity, oxidized, unmelted and semi-melted particles, inclusions, crack-like flaws and inclusions [7,13,19–21]. The porosity is generally present in the thermal sprayed coating in a range between 6 and 9% [13,22]. There are not any delaminations or spalling in coatings and quite uniform and dense coatings were obtained. If there is a mismatch in mechanical and thermal properties of coating and substrate material, cracking, spalling, and delamination may occur as given in the literature [13].

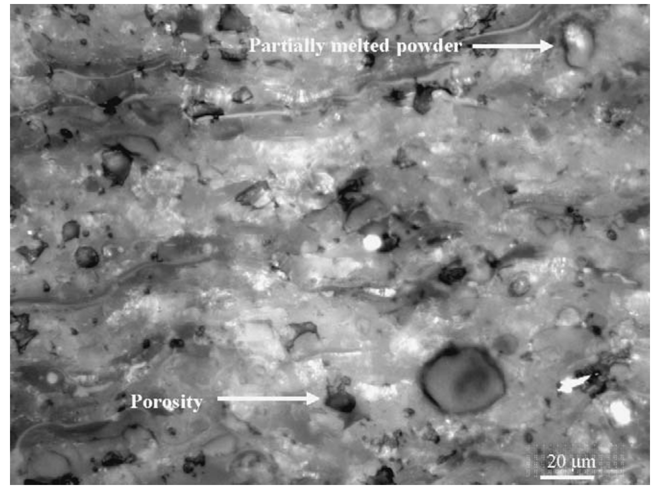

Fig. 3. Optical micrograph of cross-section view for the Al_2O_3–13 wt.% TiO_2 coating with bond coat coating deposited on titanium including porosity, partially melted ceramic powder.

3.2. XRD studies

XRD measurements of the coatings are summarized in Table 3. As mentioned by researchers [2,13,23], the Al_2O_3 coating includes γ-Al_2O_3 as major phase and α-Al_2O_3 as minor phase. Actually, the powder used in the coating contains α-Al_2O_3. Previous studies done by Li and Sun [24] also revealed that alumina coatings mainly consisted of γ-Al_2O_3. This fact suggests that the deposited spray particles have reached melting state prior to the impact on substrate. During plasma-spray process, some α-Al_2O_3 is transformed into γ-Al_2O_3 due to lower nucleation energy of this phase [20]. Previous plasma-spray studies by Goberman et al. [17] also showed that the higher critical plasma-spray parameter (CSPS) promotes the formation of γ-Al_2O_3. This observation implies that there is a good agreement with the literature and present study. The XRD

Table 3
Phases present in powders and their plasma-sprayed coatings.

Coating layer	Phases
Al_2O_3 coating	γ-Al_2O_3, α-Al_2O_3
Al_2O_3–13 wt.% TiO_2 coating	γ-Al_2O_3, α-Al_2O_3, Al_2TiO_5, TiO_2 (rutile)

analysis of Al_2O_3–13 wt.% TiO_2 coatings revealed that γ-Al_2O_3, α-Al_2O_3, Al_2TiO_5, and TiO_2 (rutile) phases are present. Al_2O_3 and TiO_2 coating powders (METCO 130 SF) are mixed and homogenized before plasma spraying to prevent agglomeration. Contact areas between two oxides are quite large due to their small powder sizes. Thus, these react together during plasma-spray process to form Al_2TiO_5. Homogenized powders also allow improving the homogeneity of the coating. A little of rutile crystallographic form of TiO_2 remained after the spraying process without reaction by Al_2O_3.

3.3. Mechanical properties

Table 4 depicts microhardness values and the depth of the layer of Al_2O_3 and Al_2O_3–13 wt.% TiO_2 coatings. The microstructure and properties of plasma-sprayed coatings generally depend on a great number of parameters, such as design of plasma torch, operating parameters including plasma arc power, plasma gases, spray distance and powder feed rate and so on [13]. As it can be seen in Table 4, the hardness of pure alumina coating is higher than that of Al_2O_3–13 wt.% TiO_2 coating. This can be attributed to the presence of titania in mixture. The microhardness values of the coatings showed that the hardness of alumina coating with bond coat is 11.40 ± 0.5 $HV_{0.1/10}$ and without bond coat is 9.50 ± 0.5 $HV_{0.1/10}$. Also, the microhardness of Al_2O_3–13 wt.% TiO_2 coating with and without bond coat is over 8.0 $HV_{0.1/10}$. The hardness of bond coat for Al_2O_3 and Al_2O_3–13 wt.% TiO_2 coatings and the substrate are 1.85 ± 0.1 $HV_{0.1/10}$, 1.70 ± 0.1 $HV_{0.1/10}$ and 1.94 ± 0.1 $HV_{0.1/10}$, respectively. The hardness of coatings is almost four times higher than that of the substrate. The hardness results indicated that the coatings with and without bond coat have a dense and uniform morphology.

The average roughness (R_a) values are given in Table 5. R_a was used to quantify the coating surface roughness. R_a is defined as the arithmetic mean of departures of the profile from the mean line. The presence of bond coat increases the surface roughness of the coating due to its coarser powder size.

Bonding strength of Al_2O_3 and Al_2O_3–13 wt.% TiO_2 coatings were tested using tensile test machine according to ASTM C 633. The bonding strength of coatings which is a mixture of cohesive and adhesive strength is summarized in Table 6. The strength of the coating layer on the substrate with bond coat is much higher than that of the coating layer formed on the substrate without bond coat. The bonding strength of Al_2O_3 and Al_2O_3–13 wt.% TiO_2 coating with bond coat are 17.64 and 28.56 MPa, respectively. Whereas, the strength of Al_2O_3 coating without bond coat is 8.97 MPa, the strength of Al_2O_3–13 wt.% TiO_2 coating without bond coat is 7.95 MPa. The results showed that the bonding strength increased in 96.65 and 259.24% of Al_2O_3 and Al_2O_3–13 wt.% TiO_2 coatings on the titanium substrate with bond coat application, respectively. It was also seen that, the dominant bonding type of Al_2O_3 and Al_2O_3–13 wt.% TiO_2 coatings with bond coat is cohesive bonding. The bond coat increases the strength of coatings and using of the bond coat on the substrate has a positive effect on mechanical performance of coatings. The bonding strength of a ceramic coating with a bonding coating is higher than that without a bonding coating [13,25]. The adhesion strength between the substrate and the ceramic coating could be improved by a NiAl bonding coating [25].

The reason for low mechanical properties without bond coat can be attributed to thermal expansion mismatch between the coating and metal substrate. It is also known that the high wettability of coating with substrate on account of bond coat increases the bonding strength between substrate and coating. The initial powder particle size of the bond coat is coarser than the initial powder size of the main coating layer of which affect contaminated surfaces and coating adhesion. In plasma-spray coating, surface roughness is also an important parameter. The adhesion strength of the impinging particle to the substrate is dependent on mechanical, metallurgical–chemical and physical mechanisms. Subsequently, diffusion or alloying may occur by forming intermetallic compounds and this is known as the metallurgical–chemical adhesion mechanism. The physical bonding is a result of particle adhesion to the substrate by Van Der Waals forces. Cohesive strength depends on the roughness, temperature difference and bond/cohesive strength of the previously coated surface [26]. It was observed that the bond coat increased the surface roughness, because of the particle sizes of bond coat powders being relatively large. Also, the surface roughness of Al_2O_3–13 wt.% TiO_2 was higher than that of pure Al_2O_3 coating which resulted in higher bonding strength. This can be attributed to the initial powder particle sizes. The bond coat having coarser particles produced less contaminated surfaces and a higher degree of the coating adhesion to the substrate. In the process, if the initial bond coat powder size is higher than that of the main coating powder size, the less contaminated surfaces would be realized and a higher degree of the coating adhesion to substrate would be observed [13].

Table 4
The variation of hardness and depth of coating with and without bond coat.

Coatings	Microhardness (GPa) ($HV_{0.1/10}$)	Layer thickness (μm)
Al_2O_3 with bond coat		
Top coat	11.40 ± 0.5	608 ± 65
Bond coat	1.85 ± 0.1	193 ± 23
Al_2O_3 without bond coat	9.50 ± 0.5	653 ± 71
Al_2O_3–13 wt.% TiO_2 with bond coat		
Top coat	8.10 ± 0.3	447 ± 38
Bond coat	1.70 ± 0.1	185 ± 25
Al_2O_3–13 wt.% TiO_2 without bond coat	8.0 ± 0.3	437 ± 31

Table 5
The surface roughness of coatings (R_a).

Coatings	R_a (μm)
Pure Al_2O_3 without bond coat	2.6 ± 0.1
Pure Al_2O_3 with bond coat	3.5 ± 0.2
Al_2O_3–13 wt.% TiO_2 without bond coat	2.8 ± 0.1
Al_2O_3–13 wt.% TiO_2 with bond coat	3.9 ± 0.2

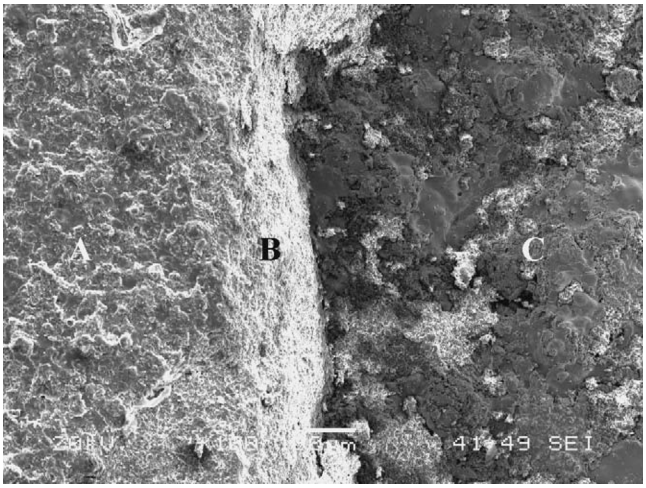

Fig. 4. SEM morphology of Al_2O_3 coating with bond coat after adhesion test. (A) Main coating, (B) failure interface, and (C) substrate.

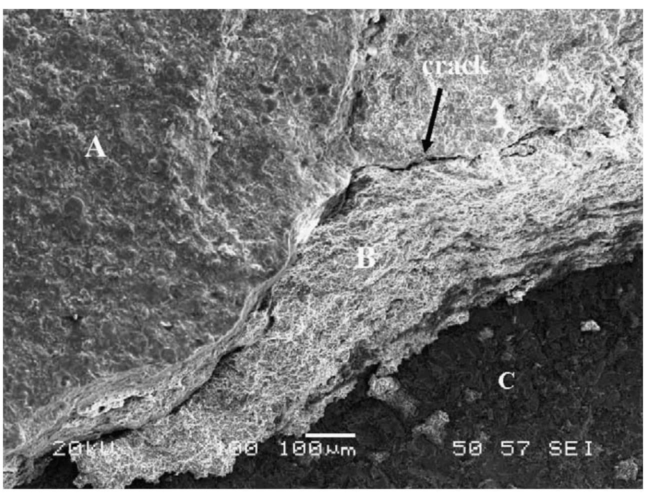

Fig. 5. SEM morphology of Al_2O_3–13 wt.% TiO_2 coating without bond coat after adhesion test. (A) Main coating, (B) failure interface, and (C) substrate.

The bonding strength of plasma-sprayed coatings is a mixture of cohesive and adhesive strength. It is well known that the bonding strength of plasma-sprayed coatings depends on the thickness of ceramic coating, the cohesive strength of the coating, surface condition, glue type and coating characteristics. It was observed that approximately the bonding type of Al_2O_3 coating without bond coat 73.41% adhesive and 26.59% cohesive character, whereas with bond coat 7.43% adhesive and 92.57% cohesive nature for same coating. For Al_2O_3–13 wt.% TiO_2 coating without bond coat, the bonding type of coating 68.04% adhesive and 31.96% cohesive, while with bond coat 7.63% adhesive and 92.37% cohesive nature for same coating. There is a good agreement with SEM micrograph of failure surfaces after adhesion test (Figs. 4 and 5) and statistical results. SEM micrograph given in Fig. 4 reflects failure in the delamination form for Al_2O_3 coated samples with bond, whereas Fig. 5 shows failure between the main coating and substrate interface including some microcracks.

Table 6
The variation of adhesion and cohesion strength of coatings.

Coatings	Bonding strength (MPa)	The bonding type of coating	
		Adhesive (%)	Cohesive (%)
Al_2O_3 without bond coat	8.97	73.41	26.59
Al_2O_3 with bond coat	17.64	7.43	92.57
Al_2O_3–13 wt.% TiO_2 without bond coat	7.95	68.04	31.96
Al_2O_3–13 wt.% TiO_2 with bond coat	28.56	7.63	92.37
Epoxy	50.31		

4. Conclusions

It is observed that it is possible to coat Al_2O_3 and Al_2O_3–13 wt.% TiO_2 on pure titanium substrate by using atmospheric plasma-spray process for determined conditions. Dense and uniform coating morphology was provided. It was seen that the hardness of coating with bond coat is higher than that of coating without bond coat. XRD analysis revealed that Al_2O_3 coating consist of γ-Al_2O_3 including little amount of α-Al_2O_3, whereas Al_2O_3–13 wt.% TiO_2 coatings revealed that γ-Al_2O_3, α-Al_2O_3, Al_2TiO_5, and TiO_2 (rutile) phases. Adhesion test results showed that the dominant type of bonding is cohesive character with bond coat.

Acknowledgments

The author would like to thank KOBATEK Company of Turkey for providing plasma spraying. The author is grateful to Sakarya University Engineering Faculty and Prof. Dr. Cuma BİNDAL, the head of the Department of Metallurgy and Material Engineering for supporting this work. The author also expresses his grateful thanks to Assoc. Prof. Dr. Uğur ŞEN and Müberra Yılmaz (MSc) for their assisting with writing, checking and experimental assistance.

References

[1] Y. Wang, S. Jiang, M. Wang, S. Wang, T.D. Xiao, P.R. Strutt, Abrasive wear characteristic of plasma sprayed nanostructured alumina/titania coatings, Wear 237 (2000) 176–185.

[2] R. Yılmaz, A.O. Kurt, A. Demir, Z. Tatlı, Effects of TiO_2 on the mechanical properties of the Al_2O_3–TiO_2 plasma sprayed coating, Journal of the European Ceramic Society 27 (2–3) (2007) 1319–1323.

[3] G. Bayrak, Ş. Yılmaz, Crystallization kinetics of plasma sprayed basalt coatings, Ceramics International 32 (2006) 441–446.

[4] C.J. Li, B. Sun, Effects of spray parameters on the microstructure and property of Al_2O_3 coatings sprayed by a low power plasma torch with a novel hollow cathode, Thin Solid Films 450 (2004) 282–289.

[5] J. Zhana, J. He, Y. Donq, X. Li, D. Yan, Microstructure characteristic of Al_2O_3–13 wt.% TiO_2 coating plasma spray deposited with nanocrystalline powders, Journal of Materials Processing Technology 197 (2008) 31–35.

[6] Ş. Yılmaz, G. Bayrak, S. Sen, U. Sen, Structural characterization of basalt-based glass–ceramic coatings, Materials and Design 27 (2006) 1092–1096.

[7] E.P. Song, J. Ahn, S. Lee, N.J. Kim, Effects of critical plasma spray parameter and spray distance on wear resistance of Al_2O_3-8 wt.% TiO_2

coatings plasma-sprayed with nanopowders, Surface and Coating Technology 202 (15) (2008) 3625–3632.

[8] P.L. Silva, J.D. Santos, F.J. Monteiro, J.C. Knowles, Adhesion and microstructural characterization of plasma sprayed hydroxyapatite/glass ceramics coatings onto Ti–6Al–4V substrates, Surface and Coating Technology 102 (1998) 191–196.

[9] Z. Mohammadi, A.A.Z. Moayyed, A.S.M. Mesgar, Grit blasting of Ti–6Al–4V alloy: optimization and its effect on adhesion strength of plasma-sprayed hydroxyapatite coatings, Journal of Materials Processing Technology 194 (2007) 15–23.

[10] S.C. Mishra, K.C. Rout, P.V.A. Padmanablan, B. Mills, Plasma sparay coating of fly ash pre-mixed with aluminium powder deposited on metal substrates, Journal of Materials Processing Technology 102 (2000) 9–13.

[11] H. Kurzweg, R.B. Heimann, T. Troczynski, M.L. Wayman, Development of plasma-sprayed bioceramic coatings with bond coats based on titania and zirconia, Biomaterials 19 (1998) 1507–1511.

[12] G. Göller, The effect of boand coat on mechanical properties of plasma sprayed bioglass–titanium coatings, Ceramic International 30 (3) (2004) 351–355.

[13] Ş. Yılmaz, M. İpek, G.F. Çelebi, C. Bindal, The effect of bond coat on mechanical properties of plasma sprayed Al_2O_3 and Al_2O_3–13 wt.% TiO_2 coatings on AISI 316L stainless steel, Vacuum 77 (2005) 315–321.

[14] E. Verne, C.F. Valles, C.V. Brovarone, S. Spriano, C. Mosisescu, Double-layer glass–ceramic coatings on Ti_6Al_4V for dental implants, Journal of the European Ceramic Society 24 (9) (2004) 2699–2705.

[15] Y.P. Lu, M.S. Li, S.T. Li, Z.G. Wang, R.F. Zhu, Plasma-sprayed hydroxyapatite titania composite bond coat for hydroxyapatite coating on titanium substrate, Biomaterials 25 (2004) 4393–4403.

[16] F. Casadei, R. Pileggi, R. Vale, A. Matthews, Studies on a combined reactive plasma sprayed/arc deposited duplex coating for titanium alloys, Surface and Coatings Technology 201 (3–5) (2006) 1200–1206.

[17] D. Goberman, Y.H. Sohn, L. Shaw, E. Jordan, M. Gell, Microstructure development of Al_2O_3–13 wt.% TiO_2 plasma sprayed coatings derived from nanocrystalline powders, Acta Materialia 50 (5) (2002) 1141–1152.

[18] C.J. Li, G.J. Yang, A. Ohmorib, Relationship between particle erosion and lamellar microstructure for plasma-sprayed alumina coatings, Wear 260 (2006) 1166–1172.

[19] E. Çelik, C. Tekmen, I. Özdemir, H. Çetinel, Y. Karakaş, S.C. Okumuş, Effects on performance of Cr_2O_3 layers produced on Mo/cast–iron materials, Surface and Coatings Technology 174–175 (2003) 1074–1081.

[20] S.C. Okumuş, Microstructural and mechanical characterization of plasma sprayed Al_2O_3–TiO_2 composite ceramic coating on Mo/cast iron substrates, Materials Letters 59 (26) (2005) 3214–3220.

[21] Z. Yin, S. Tao, X. Zhoua, C. Ding, Particle in-flight behavior and its influence on the microstructure and mechanical properties of plasma-sprayed Al_2O_3 coatings, Journal of the European Ceramic Society 28 (2008) 1143–1148.

[22] V. Fervel, B. Normand, C. Coddet, Tribological behaviour of plasma sprayed Al_2O_3–based cermet coatings, Wear 230 (1999) 70–77.

[23] X. Lin, Y. Zeng, W.S. Lee, C. Ding, Characterization of alumina–3 wt.% titania coating prepared by plasma spraying of nanostructured powders, Journal of the European Ceramic Society 24 (2004) 627–634.

[24] C.J. Li, B. Sun, Effects of spray parameters on the microstructure and property of Al_2O_3 coatings sprayed by a low power plasma torch with a novel hollow cathode, Thin Solid Films 450 (2) (2004) 282–289.

[25] S. Salman, R. Köse, L. Urtekin, F. Fındık, An investigation of different ceramic coating thermal properties, Materials and Design 27 (2006) 585–590.

[26] O. Culha, E. Çelik, N.F. Ak Azem, I. Birlik, M. Toparlı, A. Türk, Microstructural, thermal and mechanical properties of HVOF sprayed Ni–Al-based bond coatings on stainless steel substrate, Journal of Materials Processing Technology 204 (1–3) (2008) 221–230.